Journal of Alloys and Compounds 488 (2009) 294–299

Contents lists available at ScienceDirect

Journal of Alloys and Compounds

journal homepage: www.elsevier.com/locate/jallcom

# Investigations on the effects of $CoO_x$ to $MoO_x$ ratio and $CoO_x$–$MoO_x$ loading on methane decomposition into carbon nanotubes

Siang-Piao Chai[a,b], Wei-Ming Yeoh[a], Kim-Yang Lee[a], Abdul Rahman Mohamed[a,*]

[a] School of Chemical Engineering, Engineering Campus, Universiti Sains Malaysia, Seri Ampangan, 14300 Nibong Tebal, S.P.S. Pulau Pinang, Malaysia
[b] School of Engineering, Monash University, Jalan Lagoon Selatan, 46150 Bandar Sunway, Selangor, Malaysia

ARTICLE INFO

*Article history:*
Received 17 April 2009
Received in revised form 22 August 2009
Accepted 25 August 2009
Available online 31 August 2009

*Keywords:*
Carbon nanotubes
Methane decomposition
Catalysis
$CoO_x$–$MoO_x$/$Al_2O_3$
Electron microscopy

ABSTRACT

The effects of $CoO_x$ to $MoO_x$ ratio and loading amount of $CoO_x$–$MoO_x$ for $Al_2O_3$ supported catalysts on methane decomposition into carbon nanotubes (CNTs) were investigated. The reaction was performed in a fixed-bed vertical reactor at 700 °C. It has been shown that a small amount of molybdenum added brought about considerable increases in carbon yield. The highest carbon yield was recorded for the catalyst $CoO_x$:$MoO_x$ with weight ratio of 8:2. The examination of catalyst activity and carbon morphology reveals that an increase in the molybdenum content reduced the carbon yield and formed CNTs of smaller diameter and narrower diameter distribution. The study also shows that $CoO_x$–$MoO_x$ loading determines the yield of carbon and the diameter of CNTs. The yield of carbon reached the maximum at 30 wt% loading, and subsequent increases in the loading amount decreased the yield. In addition, severe agglomeration of $CoO_x$–$MoO_x$ alloy particles for high loaded $CoO_x$–$MoO_x$-containing catalysts led to the formation of larger alloy clusters that grew CNTs with comparatively larger diameters.



## 1. Introduction

The intrinsic properties of carbon nanotubes (CNTs) make them have potential applications in fields such as quantum wires, field-effect transistors, field emitters, diodes, gas sensor, electric power storage, and conductive polymers [1]. The versatility of CNTs has attracted studies not only in growing this structure, but also on how to grow CNTs with specific architectures. After the catalytic growth of CNTs was first reported by Yacaman et al. in 1993 [2], it has been generally accepted that catalytic method holds more advantages over other synthesis methods, such as laser ablation or arc-discharge, for large-scale production of CNTs. This is attributable to catalytic growth which involves simple equipment setup, lower reaction temperature and higher nanotube yields.

There are many articles which reported the influences of catalyst components on effective cracking of hydrocarbon gases into CNTs [3–6]. The compatibility of the catalyst components in growing CNTs, including the active metal, promoter and support, is indeed unique. Transition metals, such as Co, Ni or Fe, are commonly used to catalyze the growth of CNTs in catalytic chemical vapor deposition. It is well known that catalyst promoters play role in increasing both the carbon yield and the selectivity for the formation of the specific nanotube morphology, all of which are lacking in individual metals. Possible promoters, including Fe, Co, Mn, Mg, Al, Ni, Mo, Cu, Pd, Pt, etc., have been studied in decomposition process for CNTs production [3,6–14]. In our previous findings, $MoO_x$ was found to be an effective promoter for $CoO_x$ used for producing CNTs of better morphology and yield [15]. Particularly relevant to the current work, the significance of Co–Mo catalysts supported on various oxides for the synthesis of CNTs has also been reported by other research groups lately [16–22]. Co–Mo catalysts have effectively been used to grow single-walled carbon nanotubes from carbon monoxide [20,21] or alcohol [22]. It is known that a promoter can alter the morphology of active metal to suit the growth of CNTs or anticipate in enhancing or weakening metal–support interaction of the catalyst system, indirectly participating in the catalytic growth of CNTs. For this reason, the ratio of active metal to promoter is crucial and it is believed that an optimum ratio will give the highest rate of CNTs formation [9]. On the other hand, it is also widely accepted that active metal is the main component of catalyst that controls the diameter of the CNTs and the loading amount of the metal determines the size distribution of the active metal [23,24]. Thus, the influence of metal loading on the size of CNTs is identified as an important parameter to be optimized in CNTs synthesis.

Our previous studies also divulge that calcination and reduction temperature for $CoO_x$–$MoO_x$/$Al_2O_3$ catalysts has significant effects on carbon yield, quality and morphology of the CNTs obtained from methane decomposition and the suitable calcination and reduction

* Corresponding author. Tel.: +60 4 5996410.
*E-mail address:* chrahman@eng.usm.my (A.R. Mohamed).

0925-8388/$ – see front matter © 2009 Elsevier B.V. All rights reserved.
doi:10.1016/j.jallcom.2009.08.119

temperatures for the catalysts had been identified and reported [25,26]. In the present work, the influences of $MoO_x$ and the loading of $CoO_x$–$MoO_x$ on $Al_2O_3$ on the morphology of the synthesized CNTs and yield are examined. The characteristics of the catalysts and the nanotube products are studied using XRD and TEM. The preferred ratio of $MoO_x$ to $CoO_x$ and loading amount of $CoO_x$–$MoO_x$ for methane decomposition into CNTs is also reported in this paper.

## 2. Experimental

The precursors used for preparation of $MoO_x$ and $CoO_x$ were ammonium molybdate ($(NH_4)_6Mo_7O_{24}{\cdot}4H_2O$) and cobalt nitrate ($Co(NO_3)_2{\cdot}6H_2O$). $Al_2O_3$ was used as a support for $CoO_x$–$MoO_x$ catalysts. The right amount of metal nitrates was first dissolved in distilled water and then the solution was impregnated onto the $Al_2O_3$ powder. The mixture was stirred until it formed a homogeneous paste. The resulting paste was dried overnight in an oven at 105 °C, and calcined at 600 °C for 5 h. The calcined catalysts were sieved to a size of 425–600 μm. The catalysts were used without prior reduction in hydrogen flow. For investigating the effects of $MoO_x$, the ratios of $CoO_x$ to $MoO_x$ were set at 9:1, 8:2, 7:3, 6:4, 5:5, 4:6 and 2:8 (w/w) and the total metal oxide ($CoO_x$–$MoO_x$) loaded on $Al_2O_3$ was fixed at 10 wt%. In this paper, the catalyst with ratio $CoO_x$ to $MoO_x$ of 9:1 is written in the form of $9CoO_x$–$1MoO_x/Al_2O_3$. The amount of catalysts used for each run was 0.2 g and the reaction was carried out for 90 min. For investigating the effect of $CoO_x$–$MoO_x$ loading, the loading amounts of $CoO_x$–$MoO_x$ were varied from 5 to 70 wt%. High loaded $CoO_x$–$MoO_x$-containing catalysts were extremely active in methane decomposition and it resulted in a high rate of carbon formation that caused the reactor to clog, thus creating a rapid pressure buildup in the system. To prevent this problem from occurring, the amount of catalyst used in this section was reduced to 0.1 g. The reaction time was extended to 180 min after taking into consideration the longer catalytic lifetime of the high loaded $CoO_x$–$MoO_x$-containing catalysts.

Decomposition of methane over the developed catalytic materials was carried out by contacting with a mixture of methane and nitrogen at ratio 1:1 (v/v) at 700 °C in a vertical reactor. During the reaction, a part of the gases in the stream out of the catalyst bed was sampled out and analyzed by using an online gas chromatography (Hewlett-Packard Series 6890). The amount of carbon deposited was estimated from the amount of hydrogen produced, by assuming that the reaction proceeds stoichiometrically ($CH_4 \rightarrow C + 2H_2$). Carbon yield is defined as the weight of carbon deposited on the catalysts over the weight of $CoO_x$–$MoO_x$ portion in the catalyst. The detailed experimental procedures and equipment setup were reported previously [25–27]. The carbons deposited on the catalysts were analyzed using transmission electron microscope (TEM) (Philips CM12) and field emission scanning electron microscope (FESEM) (LEO Supra 50 VP). The outer diameters of the produced CNTs were measured from the respective TEM images. More than 100 CNTs per sample were taken into account for measuring their outer diameters. XRD patterns of the fresh catalysts were measured by Siemens D-5000 diffractometer, using Cu Kα radiation and a graphite secondary beam monochromator. Intensity was measured by step scanning in the $2\theta$ range of 10–90° with a step of 0.02° and a measuring time of 2 s per point.

## 3. Results and discussion

### 3.1. Effect of $CoO_x$ to $MoO_x$ ratio

Fig. 1 illustrates carbon yields of $CoO_x$–$MoO_x/Al_2O_3$ catalyst with different $CoO_x$ to $MoO_x$ ratio in methane decomposition at 700 °C. From the figure, it can be seen that a small amount of molybdenum species added to $CoO_x/Al_2O_3$ catalyst increased the yield of carbon. It was found that when the ratios of $CoO_x$ to $MoO_x$ were 9:1, 8:2, 7:3, 6:4 and 5:5 (w/w), the carbon yields obtained were higher than those of $CoO_x/Al_2O_3$ catalyst (written as $CoO_x$:$MoO_x$ = 10:0 in the paper). The maximum carbon yield, being 281%, was obtained over $CoO_x$–$MoO_x/Al_2O_3$ catalyst with ratio 8:2 (w/w). Loading of an excessive amount of $MoO_x$ decreased the yield of carbon. The catalyst with $CoO_x$ to $MoO_x$ ratio of 2:8 (w/w) was completely inactive for decomposing methane. This is expected because molybdenum is catalytically inactive in CNTs formation [28].

Fig. 2 (Left) shows the diameter distributions and (right) the TEM images of CNTs grown on $CoO_x$–$MoO_x/Al_2O_3$ catalysts with different $CoO_x$ to $MoO_x$ ratio. The TEM analysis discloses that the morphology of CNTs grown on $9CoO_x$–$1MoO_x/Al_2O_3$ catalyst was almost similar to that of CNTs grown on $8CoO_x$–$2MoO_x/Al_2O_3$ catalyst. Detailed examination of the CNTs revealed that a further

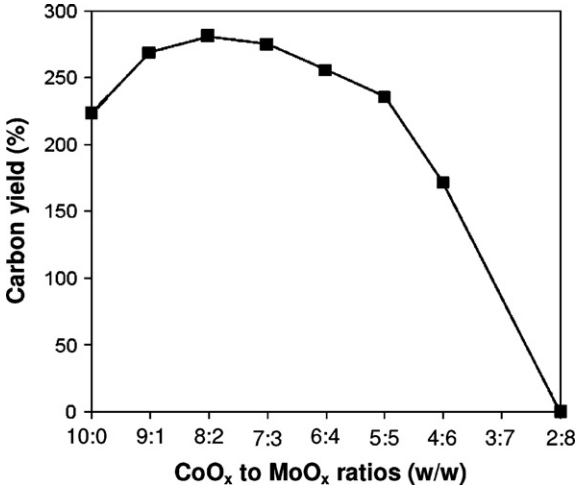


**Fig. 1.** Carbon yields in methane decomposition over $CoO_x$–$MoO_x/Al_2O_3$ catalysts with different weight ratios of $CoO_x$ to $MoO_x$ at 700 °C.

increase in the $MoO_x$ content apparently led to the formation of CNTs with a certain level of wavy structure. In this case, an excessive amount of $MoO_x$ loaded had probably altered the growth direction of CNTs at times, resulting in the formation of the wavy wall structure as observed in this study. An examination of the diameter distribution indicated that CNTs grown on $CoO_x$–$MoO_x/Al_2O_3$ catalysts with ratios of $CoO_x$ to $MoO_x$ set at 9:1, 8:2, 7:3, 6:4 and 4:6 (w/w) had the diameters of $11.3 \pm 3.4$, $10.6 \pm 3.3$, $10.7 \pm 3.5$, $9.4 \pm 3.5$ and $7.2 \pm 3.1$ nm (average ± standard deviation), respectively. An increase in the $MoO_x$ content formed CNTs with smaller diameter. Interestingly, the standard deviations of the above-mentioned CNTs were not much varied except for those grown on the catalyst with $CoO_x$ to $MoO_x$ ratio of 4:6 (w/w) which possessed slightly smaller standard deviation.

The XRD patterns of catalyst with different $CoO_x$ to $MoO_x$ ratios are shown in Fig. 3. The representative peaks for $Co_3O_4$, $CoMoO_4$, $Al_2O_3$ and $MoO_3$ are denoted in the XRD spectra. Apparently, no obvious diffraction peak for $MoO_3$ was found in Fig. 3a. This phenomenon arose either because the $MoO_3$ was well dispersed in the bulk of $CoO_x/Al_2O_3$ or the $MoO_3$ amount was too minimal to be detected by the XRD. When the ratios of $CoO_x$:$MoO_x$ were reduced to 6:4, 4:6 and 2:8 (w/w), the diffraction lines at $2\theta = 25.8°$ and 29.2° which are due to $MoO_3$ were significant (Fig. 3b–d). As we know, cobalt species is an active catalyst component and molybdenum serves as a promoter for the catalyst. Thus, decreasing the amount of $CoO_x$ and increasing the loading of $MoO_x$ reduced the yield of carbon. It is important to point out that the diffraction peaks for $CoMoO_4$ were also noted for the $MoO_x$-promoted catalyst samples. According to Hu et al., the presence of $CoMoO_4$ is important as it stabilizes the cobalt species from severe agglomeration to form larger clusters of inconsistent sizes [29]. It is evident that adding $MoO_x$ enhanced the formation of CNTs with more uniform diameter. It was also reported that unassociated $Co_3O_4$ phase or unpromoted $Co_3O_4$ would be easily reduced to metallic Co that would sinter to a larger size in the growth conditions [30]. It is well documented that CNTs could not be grown from very large sized metal particles [31,32]. Thus, this might be the cause for the carbon yields of $MoO_x$-promoted catalysts to be generally higher than those of $CoO_x/Al_2O_3$ catalyst. However, a large amount of $CoMoO_4$ formed as in $2CoO_x$–$8MoO_x/Al_2O_3$ did not contribute to methane decomposition as it can be noted that the catalyst was completely inactive in the reaction.

The surface structural model for $CoO_x/Al_2O_3$ and $CoO_x$–$MoO_x/Al_2O_3$ catalysts with different $MoO_x$ loadings were

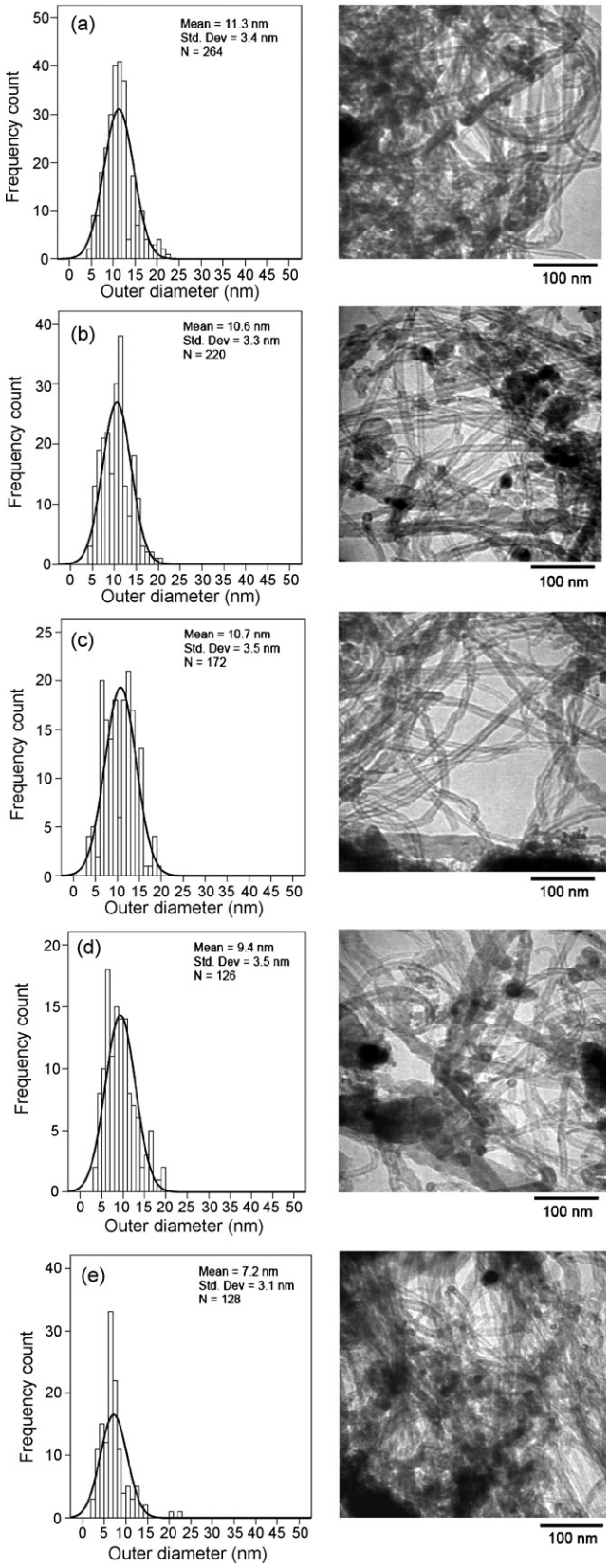


**Fig. 2.** (Left) Histograms of diameter distributions and (right) TEM images of CNTs produced on $CoO_x$–$MoO_x/Al_2O_3$ catalysts with weight ratios of $CoO_x$ to $MoO_x$ set at (a) 9:1 (w/w), (b) 8:2 (w/w), (c) 7:3 (w/w), (d) 6:4 (w/w) and (e) 4:6 (w/w).

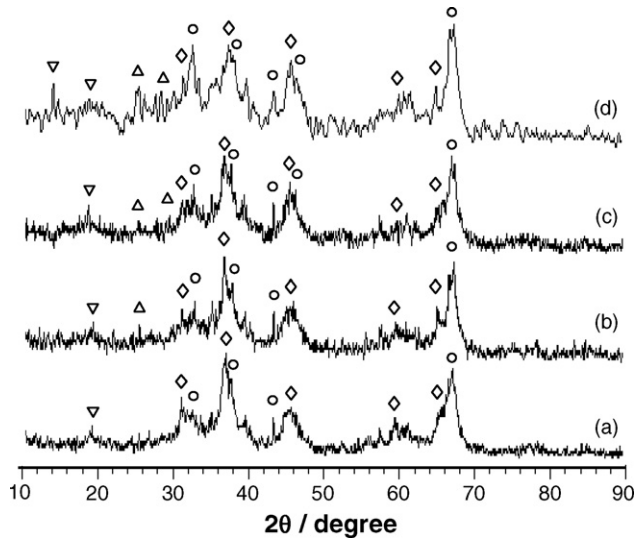


**Fig. 3.** XRD patterns of $CoO_x$–$MoO_x/Al_2O_3$ catalysts with weight ratios of $CoO_x$ to $MoO_x$ set at (a) 8:2 (w/w), (b) 6:4 (w/w), (c) 4:6 (w/w) and (d) 2:8 (w/w). (◊) $Co_3O_4$, (○) $Al_2O_3$, (▽) $CoMoO_4$, (△) $MoO_3$.

conjectured based on the findings obtained in this study and the models reported elsewhere [29,33]. The scheme for the proposed model is presented in Fig. 4. By comparing Fig. 4a and b, it is noted that cobalt species for $MoO_x$-free catalyst had various sizes, whereas $MoO_x$-promoted catalyst possessed more uniform sized $Co_3O_4$ due to the formation of $CoMoO_4$ in preventing the agglomeration of the cobalt particles. This is the reason why $MoO_x$-promoted $CoO_x/Al_2O_3$ catalyst grew more uniform diameter CNTs as shown in the TEM images. An increase in $MoO_x$ loading increased the amount of $CoMoO_4$ generated, as shown in Fig. 4c. The formation of larger sized $CoMoO_4$ crystallites could restrict and reduce the size of $Co_3O_4$ crystallites. Thus, as can be observed in the TEM images, CNTs of smaller diameter were grown on the catalyst with higher $MoO_x$ content. Unassociated $MoO_3$ crystallites were prevalent as shown in Fig. 4c. Fig. 4d illustrates the surface condition of high loaded $MoO_x$ catalyst. Large amounts of unassociated $MoO_3$ and $CoMoO_4$ crystallites were seen and only minimal $Co_3O_4$ could be traced on the surface of the catalyst. This is conjectured based on the XRD results, showing significant peaks for both $MoO_3$ and $CoMoO_4$ crystallites and a reduced peak of $Co_3O_4$ crystallites for $2CoO_x$–$8MoO_x/Al_2O_3$ catalyst (Fig. 4d). As mentioned earlier, $MoO_x$ is catalytically inactive; therefore, high loaded $MoO_x$ catalyst had reduced activity in methane decomposition.

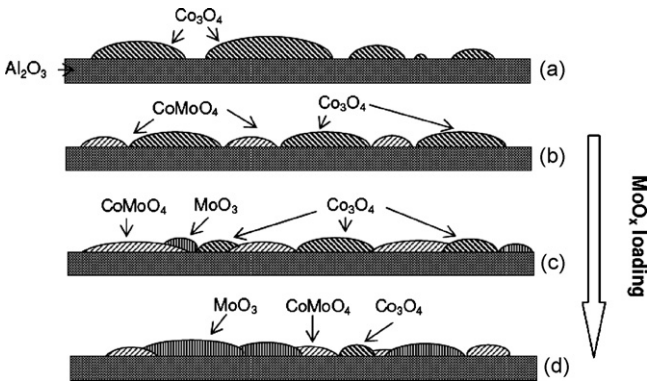


**Fig. 4.** Scheme illustrating the surface structural model proposed for (a) $CoO_x/Al_2O_3$ and (b–d) $CoO_x$–$MoO_x/Al_2O_3$ with increasing loadings of $MoO_x$.

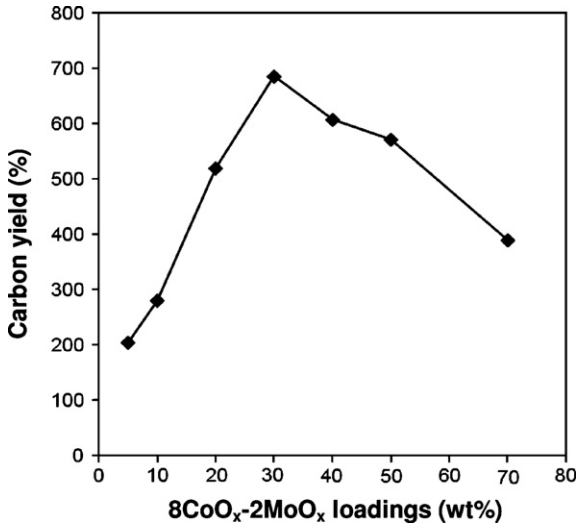


**Fig. 5.** Carbon yields in methane decomposition over $8CoO_x$–$2MoO_x/Al_2O_3$ catalyst with different loadings of $8CoO_x$–$2MoO_x$ at 700 °C.

### 3.2. Effect of $CoO_x$–$MoO_x$ loading amount

As a consequence of the highest carbon yield was obtained for the catalyst with $CoO_x$ to $MoO_x$ ratio of 8:2 (w/w), investigations on the effect of $CoO_x$–$MoO_x$ loading on alumina with respect to carbon yield and the morphology of CNTs were carried out for $8CoO_x$–$2MoO_x/Al_2O_3$ catalyst. Fig. 5 shows the carbon yields of catalysts with different loadings of $8CoO_x$–$2MoO_x$ from methane decomposition at 700 °C. Obviously, carbon yields increased remarkably with an increase in the loadings of $8CoO_x$–$2MoO_x$ from 5 to 30 wt%. The yield reached a maximum of 686% at 30 wt%. This is explicable because more active sites for the reaction were provided by a catalyst with increasing amount of active component. However, further increase in the loadings of $8CoO_x$–$2MoO_x$ from 30 to 70 wt% resulted in decreasing yield of carbon.

Fig. 6 (Left) shows diameter distribution histograms and (right) TEM images of the produced CNTs. Apparently, as the metal oxide loading increased, the grown CNTs possessed larger diameters, as marked with arrows in Fig. 6. From the aspect of diameter distribution, the catalysts that were loaded with 5 and 10 wt% of $8CoO_x$–$2MoO_x$ grew CNTs with comparatively narrower diameter distributions, i.e. $6.6 \pm 2.8$ nm (Fig. 6a) and $10.6 \pm 3.3$ nm (Fig. 6b), respectively. The average diameter of CNTs produced on the catalyst with 5 wt% loading was obviously smaller than that produced on 10 wt% loading. The catalyst with 20 wt% loading saw the growth of CNTs with much larger diameter and wider diameter distribution ($13.1 \pm 8.1$ nm), as shown in Fig. 6b. CNTs with diameters larger than 40 nm were also found on the said catalyst. Fig. 6c demonstrates that the average diameter and standard deviation of the CNTs formed on the catalyst with 30 wt% loading of $8CoO_x$–$2MoO_x$ were 17.9 and 13.9 nm, respectively. An increase in $8CoO_x$–$2MoO_x$ loading to 50 wt% led to the formation of CNTs with comparatively larger diameter and wider distribution, i.e. $21.0 \pm 19.3$ nm (Fig. 6d). Some of the CNTs were found with diameters larger than 100 nm. Fig. 6e shows the diameter distribution and TEM image of CNTs formed on the catalyst loaded with 70 wt% of $8CoO_x$–$2MoO_x$. It was observed that the formed CNTs had diameters ranging from 6 to 114 nm with an average diameter of 24.0 nm and standard deviation of 21.4 nm. An obvious trend was observed when examining the diameter distribution of the grown CNTs with respect to the metal oxide loadings. It shows that an increase in the loading resulted in the growth of CNTs with increasing average diameter and diameter distribution. Although 30 wt% loading gave the high-

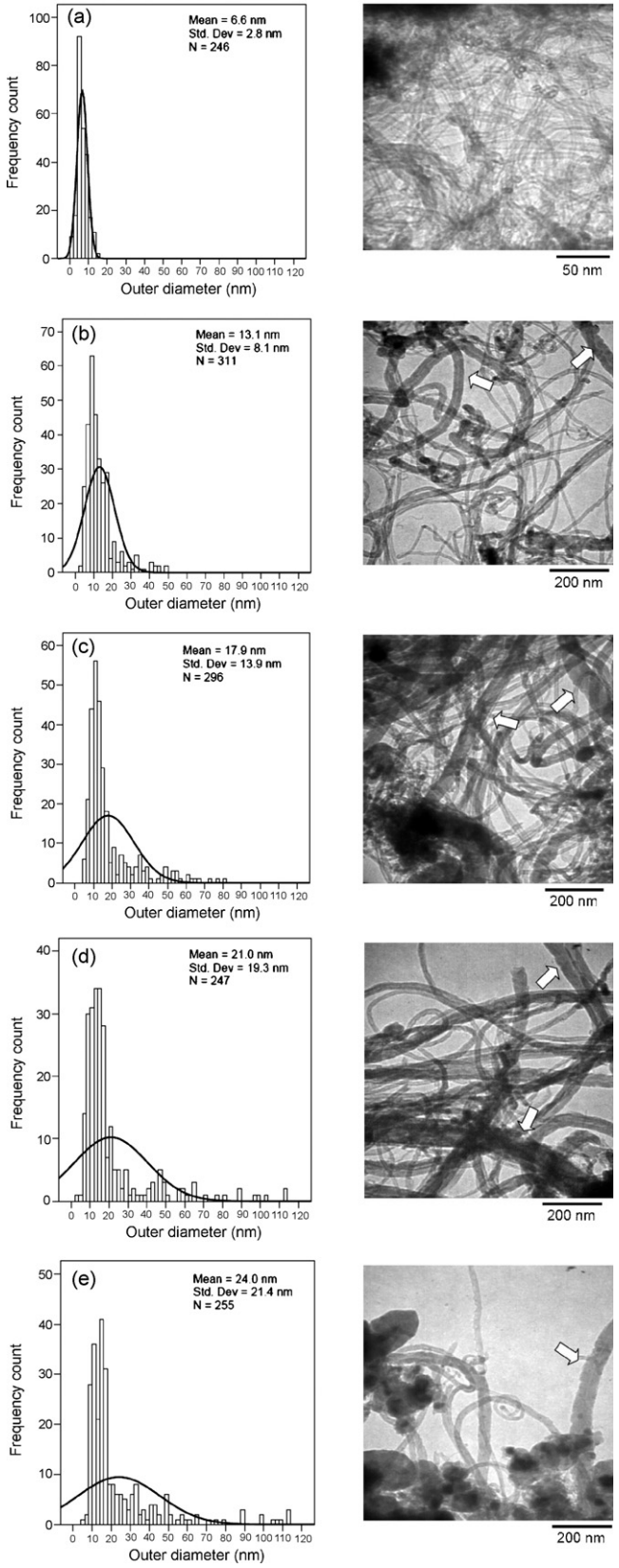


**Fig. 6.** (Left) Histograms of diameter distributions of CNTs and (right) TEM images of CNTs grown on $8CoO_x$–$2MoO_x/Al_2O_3$ catalysts with $8CoO_x$–$2MoO_x$ loadings of (a) 5 wt%, (b) 20 wt%, (c) 30 wt%, (d) 50 wt% and (e) 70 wt%.

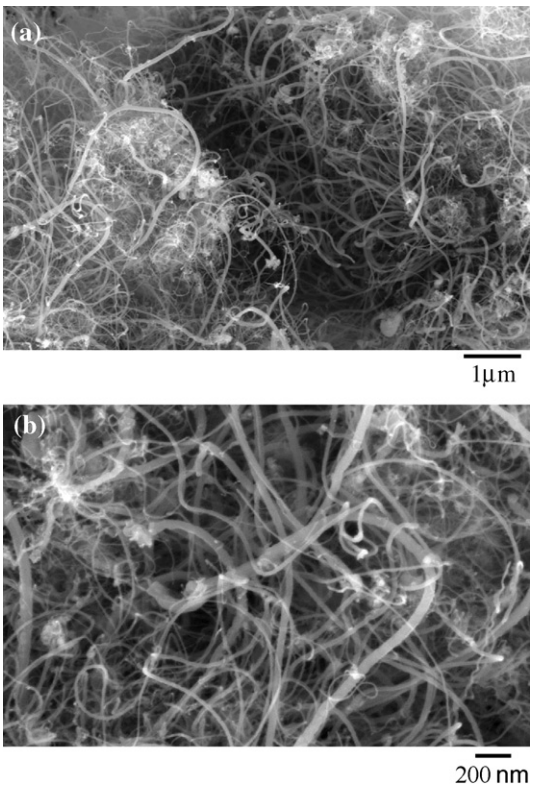


**Fig. 7.** (a) Low-magnified and (b) high-magnified SEM images of CNTs grown on $8CoO_x$–$2MoO_x/Al_2O_3$ catalyst with 30 wt% of $8CoO_x$–$2MoO_x$.

est yield of carbon, the 5 wt% loading grew CNTs of the narrowest diameter distribution. Fig. 7 shows the low-magnified and high-magnified SEM images of the CNTs grown on the catalyst loaded with 30 wt% of $8CoO_x$–$2MoO_x$.

The XRD patterns of $8CoO_x$–$2MoO_x/Al_2O_3$ catalyst with different loadings are shown in Fig. 8. Characteristic peaks of $Co_3O_4$, $CoMoO_4$ and $Al_2O_3$ are indicated in the diffractograms. In Fig. 8a and b, the broad peak of $Co_3O_4$ at $2\theta = 36.8^\circ$ revealed that smaller sized $Co_3O_4$ crystallites were formed on $Al_2O_3$ support for the catalyst with 5 and 10 wt% of $8CoO_x$–$2MoO_x$ loading. It is markedly noted that the intensity of peak at 36.8° was greater and the width of the peak became narrower with the increase in the $8CoO_x$–$2MoO_x$ loading (Fig. 8c–e). This is due to the fact that larger sized $Co_3O_4$ crystallites were formed on the $Al_2O_3$ support for high loaded $8CoO_x$–$2MoO_x$-containing catalyst. The average sizes of $Co_3O_4$ crystallites as estimated from peak $2\theta = 36.8^\circ$ using Scherrer's equation are tabulated in Table 1. It can be seen that the size of the $Co_3O_4$ crystallites increased with the increasing loading of $8CoO_x$–$2MoO_x$. It is speculated that as the loadings were increased, some of the $8CoO_x$–$2MoO_x$ crystallites might have agglomerated with the adjacent crystallites, forming $8CoO_x$–$2MoO_x$ alloys which more of inconsistent sizes but comparatively larger than those of the catalyst with small metal oxide loading. The formation of these clusters could lead to the growth of CNTs of larger diameter and wider diameter distribution. Moreover, it was mentioned earlier that CNTs could not be grown from very large sized metal particles [31,32]. Thus, it is strongly believed that the failure in the formation of CNTs on the catalyst with larger alloy clusters for high loaded $CoO_x$–$MoO_x$-containing catalysts contributed to the increase in the surface carbon deposition, leading to encapsulation of the active sites by the deposited surface carbon, thus deactivating the catalyst. This explains well the decreasing trend of carbon yields observed for the catalysts of more than 30 wt% loadings.

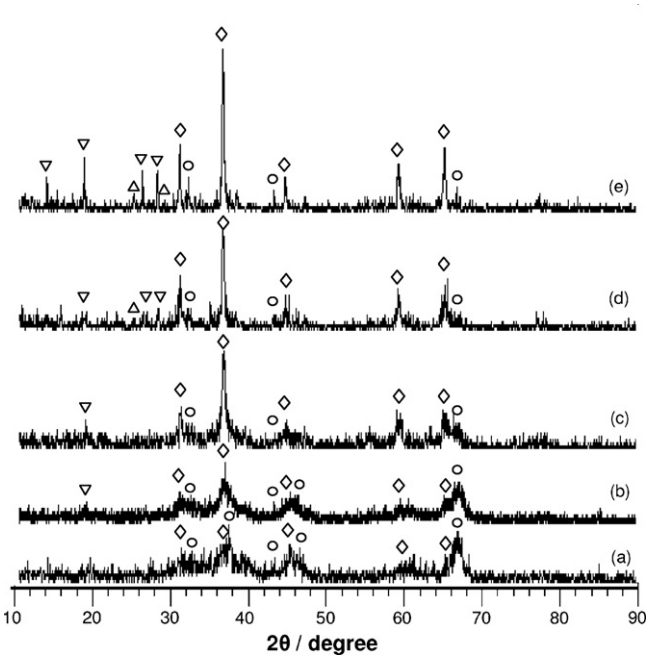


**Fig. 8.** XRD patterns of $8CoO_x$–$2MoO_x/Al_2O_3$ catalysts with $8CoO_x$–$2MoO_x$ loadings of (a) 5 wt%, (b) 10 wt%, (c) 30 wt%, (d) 50 wt% and (e) 70 wt%, respectively. (◊) $Co_3O_4$, (○) $Al_2O_3$, (▽) $CoMoO_4$, (△) $MoO_3$.

**Table 1**
The average sizes of cobalt oxide crystallites for different loadings of $8CoO_x$–$2MoO_x$.

| Sample | $8CoO_x$–$2MoO_x$ (wt%) | Average $Co_3O_4$ crystallite size (nm) |
|---|---|---|
| 1 | 5 | 4.7 |
| 2 | 10 | 6.3 |
| 3 | 30 | 17.7 |
| 4 | 50 | 23.8 |
| 5 | 70 | 26.2 |

## 4. Conclusions

The role of molybdenum in bimetallic $CoO_x$–$MoO_x/Al_2O_3$ catalyst is of importance as it assisted in increasing the yield of CNTs and growing CNTs with more uniform diameter. The findings show that an increase in $MoO_x$ content grew smaller diameter CNTs, resulting from the restriction of $CoMoO_4$ on the size of $Co_3O_4$ crystallites. A further increase in $MoO_x$ loading reduced the carbon yield due to the substitution of active cobalt by inactive molybdenum. The optimum ratio of $CoO_x$ to $MoO_x$ was found to be 8:2 (w/w), a ratio that produced higher yield. The findings also reveal that $MoO_x$ was an effective promoter for $CoO_x/Al_2O_3$ catalyst only when the amount added was small and adding an excessive amount of $MoO_x$ is not encouraged as it brought about reduced catalytic activity and lowered carbon yield. The performance of the catalyst in methane decomposition into CNTs depended highly on the loading amount of $CoO_x$–$MoO_x$, suggesting that the growth of CNTs could be related to the particle size of the alloys. In addition, the size of the particles determines the diameter of the nanotubes as it can be seen that the catalyst loaded with high content of $CoO_x$–$MoO_x$ grew CNTs of larger diameter. The total metal oxide loading at 30 wt% on alumina support gave the highest yield of carbon. Subsequent increases the loading reduced the yield. It is reasonable to speculate that the alloy particles of high loaded $CoO_x$–$MoO_x$-containing catalysts can easily agglomerate to form larger clusters which are not suitable for growing CNTs, thus causing an increase in the surface carbon accumulation and eventually deactivating the catalyst.

## Acknowledgements

This work was supported by the Universiti Sains Malaysia (USM) under the Research University Grant Scheme (Project A/C No. 814004) and the Malaysian Technology Development Corporation (MTDC) under the Commercialization of Research & Development Fund (CRDF) (Project A/C No. MBF065-USM/05).

## References

[1] R.H. Baughman, A.A. Zakhidov, W.A. de Heer, Science 297 (2002) 787–792.
[2] M.J. Yacaman, M.M. Yoshida, L. Rendon, J.G. Santiesteban, Appl. Phys. Lett. 62 (1993) 202–204.
[3] Q. Zhang, W. Qian, Q. Wen, Y. Liu, D. Wang, F. Wei, Carbon 45 (2007) 1645–1650.
[4] H.-A. Ichi-oka, N.-O. Higashi, Y. Yamada, T. Miyake, T.T. Suzuki, Diam. Relat. Mater. 16 (2007) 1121–1125.
[5] F.E. Trigueiro, C.M. Ferreira, J.C. Volta, W.A. Gonzalez, P.G.P. de Oliveria, Catal. Today 118 (2006) 425–432.
[6] A.-C. Dupuis, Prog. Mater. Sci. 50 (2005) 929–961.
[7] Y. Li, X.B. Zhang, X.Y. Tao, J.M. Xu, W.Z. Huang, J.H. Luo, Z.Q. Luo, T. Li, F. Liu, Y. Bao, H.J. Geise, Carbon 43 (2005) 295–301.
[8] S.H.S. Zein, A.R. Mohamed, Energy Fuels 18 (2004) 1336–1345.
[9] S. Takenaka, Y. Shigeta, E. Tanabe, K. Otsuka, J. Catal. 220 (2003) 468–477.
[10] X. Li, Y. Zhang, K.J. Smith, Appl. Catal. A 264 (2004) 81–91.
[11] T.V. Reshetenko, L.B. Avdeeva, V.A. Ushakov, E.M. Moroz, A.N. Shmakov, V.V. Kriventsov, D.I. Kochubey, Y.T. Pavlyukhin, A.L. Chuvilin, Z.R. Ismagilov, Appl. Catal. A 270 (2004) 87–99.
[12] J. Chen, Y. Li, Z. Li, X. Zhang, Appl. Catal. 269 (2004) 179–186.
[13] S.-P. Chai, W.-W. Liu, K.-Y. Lee, W.-M. Yeoh, V.M. Sivakumar, A.R. Mohamed, Mater. Lett. 63 (2009) 1428–1430.
[14] M. Escobar, G.H. Rubiolo, M.S. Moreno, S. Goyanes, R. Candal, J. Alloys Compd. 479 (2009) 440–444.
[15] S.-P. Chai, S.H.S. Zein, A.R. Mohamed, Chem. Phys. Lett. 426 (2006) 345–350.
[16] C. Vallés, M. Pérez-Mendoza, W.K. Maser, M.T. Martínez, L. Alvarez, J.L. Sauvajol, A.M. Benito, Carbon 47 (2009) 998–1004.
[17] Z. Niu, Y. Fang, Mater. Res. Bull. 43 (2008) 1393–1400.
[18] W.-M. Yeoh, K.-Y. Lee, S.-P. Chai, K.-T. Lee, A.R. Mohamed, New Carbon Mater. 24 (2009) 119–123.
[19] N. Ishigami, H. Ago, T. Nishi, K.-I. Ikeda, M. Tsuji, T. Ikuta, K. Takahashi, J. Am. Chem. Soc. 130 (2008) 17264–17265.
[20] V.M. Irurzun, Y. Tan, D.E. Resasco, Chem. Mater. 21 (2009) 2238–2246.
[21] B. Wang, Y. Yang, L.-J. Li, Y. Chen, J. Mater. Sci. 44 (2009) 3285–3295.
[22] H. Sugime, S. Noda, S. Maruyama, Y. Yamaguchi, Carbon 47 (2009) 234–241.
[23] R.T.K. Baker, Carbon 27 (1989) 315–323.
[24] S. Takenaka, S. Kobayashi, H. Ogihara, K. Otsuka, J. Catal. 217 (2003) 79–87.
[25] S.-P. Chai, S.H.S. Zein, A.R. Mohamed, Carbon 45 (2007) 1535–1541.
[26] S.-P. Chai, S.H.S. Zein, A.R. Mohamed, Appl. Catal. A 326 (2007) 173–179.
[27] S.-P. Chai, S.H.S. Zein, A.R. Mohamed, Diam. Relat. Mater. 16 (2007) 1656–1664.
[28] Y. Murakami, S. Chiashi, Y. Miyauchi, S. Maruyama, Jpn. J. Appl. Phys. 43 (2004) 1221–1226.
[29] M. Hu, Y. Murakami, M. Ogura, S. Maruyama, T. Okubo, J. Catal. 225 (2004) 230–239.
[30] J.E. Herrera, D.E. Resasco, J. Catal. 221 (2004) 354–364.
[31] L.B. Avdeeva, O.V. Goncharova, D.I. Kochubey, V.I. Zaikovskii, L.M. Plyasova, B.N. Novgorodov, S.K. Shaikhutdinov, Appl. Catal. A 141 (1996) 117–129.
[32] G.G. Tibbetts, J. Cryst. Growth 66 (1984) 632–638.
[33] H. Vidal, S. Bernal, R.T. Baker, D. Finol, J.A.P. Omil, J.M. Pintado, J.M. Rodriguez-Izquierdo, J. Catal. 183 (1999) 53–62.